



Numerical study on CTF code to predict void fraction in PWR sub channel conditions

Hoang Minh Giang¹, Hoang Tan Hung¹, Nguyen Phu Khanh²

¹ Nuclear Safety Center, Institute for Nuclear Science and Technology

²Hanoi University of Science and Technology

Abstract: CTF is a version of the widely used COBRA-TF code with capability of 3D simulation for core sub channel thermal hydraulics behavior. Recently, CTF is reviewed and the consideration of CTF to predict void fraction in PWR sub channel conditions such as subcooled region still need more investigation. Due to the fact that the Chen's correlation of heat transfer coefficient is developed for relatively low pressure and high quality conditions associated with forced convection vaporization, and is not strictly valid for PWR operation conditions, so that, in this study, some runs of single channel in the benchmark based on NUPEC PWR Sub channel and Bundle Tests (PSBT) are used to investigate void fraction prediction by CTF in subcooled region and also to verify some remarkable notice of CTF from other authors. The goal of the study is to evaluate deviation for CTF void fraction prediction in PWR sub channel conditions.

Keywords: CTF, COBRA-TF, void fraction, PWR, PSBT, Chen's correlation...

I. INTRODUCTION

CTF is a version of COBRA-TF code improved by Pennsylvania State University (PSU), PA, USA. The code is developed to investigate core sub channel behavior. Therefore, CTF is used to predict the PSBT single sub channel steady state [1] with all geometries: S1, S2, S3 and S4 in [2, 3] and give void fraction results within error of $\pm 10\%$ void. Furthermore, CTF investigation for EPRI Rod Bundle Tests [4,5] shows two findings: (a) the Chen's correlation for heat transfer in normal wall (non-CHF) condition used with a wide range of flow regimes would lead to inaccurate results for numerous reactor flow simulations; (b) an over prediction for liquid enthalpy, while preserving the total enthalpy for the subcooled boiling conditions. As mentioned in [4] this issue comes from an incorrect partitioning of heat input to the fluid. For normal flow regimes

(defined in CTF as $T_w < T_{CHF}$), the wall heat flux is allocated only to the liquid and it is not valid for subcooled boiling conditions.

In other hand, it is known that CFX employs RPI wall boiling model with heat flux from the wall partitioning into both liquid (convective, quenching) and vapor directly. Thus, this boiling model is differ from CTF model for subcooled region where heat flux is partitioned only into liquid phase. Additionally, CFX is simulation code with a scale smaller than CTF, so the local phenomena such as wall heat transfer may be captured more precise. Therefore, in some runs of PSBT S1 exercises, if CFX give better accurate results of average cross section void fraction in comparison with experiment, then CFX modeling may be considered to simulate appropriately the above runs. So in such case, CFX enthalpy and void distribution predictions may be used as reference to compare with CTF in these

predictions. The comparison of void fraction and enthalpy prediction distributions with experiment is impossible due to not any distribution provided from NUPEC PWR Sub channel and Bundle Tests (PSBT). So that in this study, CFX will be used to investigate some runs of PSBT single sub channel (S1) with enough accurate results in order to confirm that CFX modeling is appropriate to experiment. Thus, in such runs, CFX investigation can be used as reference to review CTF results. After that, based on (a) comparison of CTF void fraction prediction with experimentally measured data and (b) comparison of prediction on average void distribution along axial channel with the reference results given by CFX, the consideration of CTF capability for void fraction prediction in PWR sub channel will be discussed. Furthermore, the verification of CTF liquid enthalpy prediction as mentioned in [4] will be also discussed by comparison of CTF results for average liquid enthalpy distribution along axial channel with reference given by CFX.

II. PHYSICAL MODELS IN CTF AND CFX

A. CTF models for evaporation and condensation

Evaporation and condensation induced by thermal phase change

The CTF model includes nine conservation equations and three fields: liquid, vapor and entrained liquid drop. The various forms of conservation equations are presented [3, 6]. However, only ref. [3] takes into account core sub channel geometry. To determine closure models for governing equations, the flow regime maps are used to calculate the interfacial transportation terms such as momentum transfer and heat transfer terms. There are two different types of flow regime maps: “normal wall” map and “hot wall” map. The normal wall map is used when the

maximum wall surface temperature, T_w , in a given computational mesh cell is below the critical heat flux temperature, T_{crit} . Then a part of wall adjacent to this mesh cell is expected to be fully wetted. The normal wall flow regime map includes the following flow regimes: small bubble; small-to-large bubble (slug); churn/turbulent; and annular/mist.

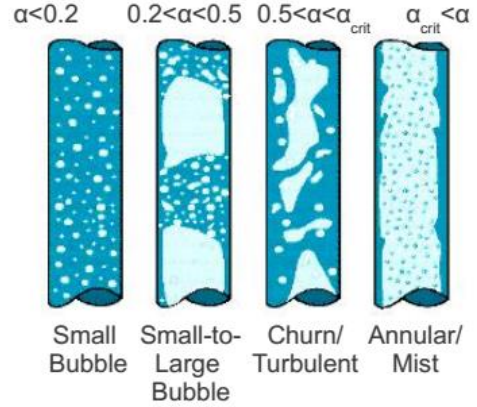


Fig. 1. CTF normal-wall flow regime map [6].

In the subcooled region, heat transfer from the wall partitioned only into liquid is given by:

$$q_w''' = h_c(T_w - T_l) \frac{A_s}{A_x \Delta X} \quad (1)$$

Where h_c is Chen correlation:

$$h_c = h_{fc} + h_{nb} \quad (2)$$

In formula (2), h_{fc} is a modified Dittus-Boelter correlation:

$$h_{fc} = 0.0023 F_{chen} \left(\frac{k_l}{D_h} \right) Re_l^{0.8} Pr^{0.4} \quad (3)$$

$$F_{chen} = \begin{cases} 1.0 & \text{if } \chi_{TT}^{-1} < 0.1 \\ 2.34(\chi_{TT}^{-1} + 0.213)^{0.736} & \text{if } \chi_{TT}^{-1} > 0.1 \end{cases} \quad (4)$$

$$\chi_{TT}^{-1} = \left(\frac{x}{1-x} \right)^{0.9} \left(\frac{\rho_l}{\rho_g} \right)^{0.5} \left(\frac{\mu_g}{\mu_l} \right)^{0.1} \quad (5)$$

The nucleate boiling heat transfer coefficient, h_{nb} , is given by:

$$h_{nb} = 0.00122S_{chen} \left(\frac{k_l^{0.79} C_{pl}^{0.45} \rho_l^{0.49} g_c^{0.25}}{\sigma^{0.5} \mu_l^{0.29} h_{lg}^{0.24} \rho_g^{0.24}} \right) (T_w - T_{sat})^{0.24} (P(T_w) - P(T_{sat}))^{0.75} \quad (6)$$

$$S_{chen} = \begin{cases} (1 + 0.12Re_{2\phi}^{1.14})^{-1} & \text{if } Re_{2\phi} < 32.5 \\ (1 + 0.42Re_{2\phi}^{0.78})^{-1} & \text{if } 32.5 < Re_{2\phi} < 50.9 \\ 0.1 & \text{if } Re_{2\phi} > 50.9 \end{cases} \quad (7)$$

$$Re_{2\phi} = (10^{-4}) Re_l F_{chen}^{1.25} \quad (8)$$

$$P(T_w) - P(T_{sat}) = \left[\frac{5.4042h_{lg}}{U_{lg}(T_{sat}+460)} \right] (T_w - T_{sat})^A \quad (9)$$

$$A = \frac{1.0306}{(\log_{10} P)^{0.017}} + \frac{0.0020632}{(\log_{10} P)^{1.087}} \max\{0.0, (T_w - T_{sat}) - 5.0\} \quad (10)$$

Whenever heat from the wall is transferred to liquid, liquid enthalpy increases and the phase change which is expressed via volumetric mass flow rate, Γ''' , is provided by:

$$\Gamma''' = \left[\frac{A'''_{int,shl} h_{i,shl}}{(h_{g,sat} - h_{l,sat}) C_{pl}} |h_l - h_{l,sat}| + \frac{A'''_{int,shv} h_{i,shv}}{(h_{g,sat} - h_{l,sat}) C_{pv}} |h_g - h_{g,sat}| \right] - \left[\frac{A'''_{int,scl} h_{i,scl}}{(h_{g,sat} - h_{l,sat}) C_{pl}} |h_l - h_{l,sat}| + \frac{A'''_{int,scv} h_{i,scv}}{(h_{g,sat} - h_{l,sat}) C_{pv}} |h_g - h_{g,sat}| \right] \quad (11)$$

Evaporation and condensation induced by turbulent mixing and void drift

Another phenomenon that can cause phase change is turbulence. The CTF's turbulent mixing and void drift uses a simple turbulent-diffusion model by calculating the lateral velocity from sub channel to sub channel. Based on the turbulent mixing model, the mass exchange of phase (k), \dot{m}_k^{TM} , induced by sub channel (i) and (j) can be defined as:

$$\dot{m}_k^{TM} = \beta_{TP} \frac{\bar{G}}{\rho} (\alpha_{kj} \rho_{kj} - \alpha_{ki} \rho_{ki}) \quad (12)$$

The mass exchange, \dot{m}_k^{VD} , due to drift model is obtained:

$$\dot{m}_k^{VD} = \beta_{TP} \frac{\bar{G}}{\rho} (\alpha_{kJEQ} \rho_{kJEQ} - \alpha_{kiEQ} \rho_{kiEQ}) A \quad (13)$$

The β_{TP} is Beus's correlation for two-phase turbulent mixing coefficient [8].

B. CFX models for evaporation and condensation

Evaporation at the wall

In the CFX, evaporation is induced directly by heat transfer from the wall. CFX employs the RPI wall partition model in which total wall heat flux, q_w'' , is divided into three components of heat flux: convective, q_c'' , queching, q_q'' and evaporative, q_e'' .

$$q_w'' = q_c'' + q_q'' + q_e'' \quad (14)$$

The evaporation rate, Γ_{gl}'' , from liquid to vapor is given by:

$$\Gamma_{gl}'' = A_2 \frac{Q_e}{(h_{g,sat} - h_l)} = A_2 \frac{\pi}{6} d_w^3 \rho_g f n \quad (15)$$

Where:

The area influence factor, A_2 , is defined by:

$$A_2 = \min(\pi d_w^2 \cdot n, 1) \quad (16)$$

The term of wall nucleation site density, n , is given by sub models:

$$n [m^{-2}] = [m(\Delta T_{sup} [K])]^p \quad (17)$$

The bubble departure diameter, d_w , is defined by Tolubinskiy sub model:

$$d_w = \min \left(d_{ref} \exp \left(-\frac{\Delta T_{sub}}{\Delta T_{ref}} \right), d_{max} \right) \quad (18)$$

The bubble detachment frequency, f , is given by Kurul and Podowski sub model:

$$f = \sqrt{\frac{4g(\rho_l - \rho_g)}{3C_D d_w \rho_l}} \quad (19)$$

Condensation model in bulk of liquid

In the CFX, vapor is always assumed in saturated condition. So that in a bulk of liquid heat is only transferred from vapor to liquid. The heat transfer per volumetric unit, Q_l , is defined by formula (20).

$$Q_l = h_{lg} A_{lg} (T_{sat} - T_l) \quad (20)$$

Where:

The interfacial area density, A_{lg} , is given by

$$A_{lg} = \frac{6rg}{d_\beta} \quad (21)$$

The heat transfer from vapor to liquid, h_{lg} , is estimated by Nusselt number:

$$h_{lg} = \frac{\lambda_l Nu_{lg}}{d_\beta} \quad (22)$$

In formulas (22) and (22) the local mean bubble diameter, d_β , is proposed by Kurul and Podowski [9] as well as Anglart et al. [10].

$$d_\beta = \frac{d_{b1}(T_{sub} - T_{sub,2}) + d_{b2}(T_{sub,1} - T_{sub})}{(T_{sub,1} - T_{sub,2})} \quad (23)$$

in which $d_{b1} = 0.1\text{mm}$ at $T_{sub,1} = 13.5\text{K}$ and $d_{b2} = 2\text{mm}$ at $T_{sub,2} = -5\text{K}$.

The Nusselt number used in the formula (22) can be chosen from several correlations such as Ranz Marshall Model:

$$Nu_{lg} = 2 + 0.6Re^{0.5}Pr^{0.3} \quad (24)$$

Recently, Nusselt correlation is proposed by Kim and Park (2011) [11]:

$$Nu_{lg} = 0.2575Re_b^{0.7}Pr_f^{-0.4564}Ja^{-0.2043} \quad (25)$$

And Warriar [2002] Nusselt correlation is also proposed in [11]:

$$Nu_{lg} = 0.6Re_b^{\frac{01}{2}}Pr_f^{\frac{1}{3}}(1 - 1.2Ja^{\frac{9}{10}}Fo_0^{\frac{2}{3}}) \quad (26)$$

III. RESULTS AND DISCUSSION

According to [1], NUPEC PSBT benchmark consists of two phases with different exercises, where the first phase focuses on void distribution benchmark with four exercises. The first exercise is steady-state single sub channel benchmark with different geometries (S1, S2, S3 and S4). Figure 2 shows the test section used for the typical center sub channel (S1) with the heated length of 1555mm and the measuring position of void fraction located at 1400mm elevation over the inlet. At cross section view, the diameter, pitch and gap of the rod are 9.5mm, 12.6mm and 3.1mm, respectively. Several runs were selected to investigate, in which pressure varies from 50 to 169 kg/cm² (see Table1). Depending on specific runs, the CFX simulation will uses different Nusselt correlations such as: Warriar, Kim and Park or Rans Mashall. The average void fraction predictions by CFX and CTF were given in Table 1 and also are presented in Figure 2.

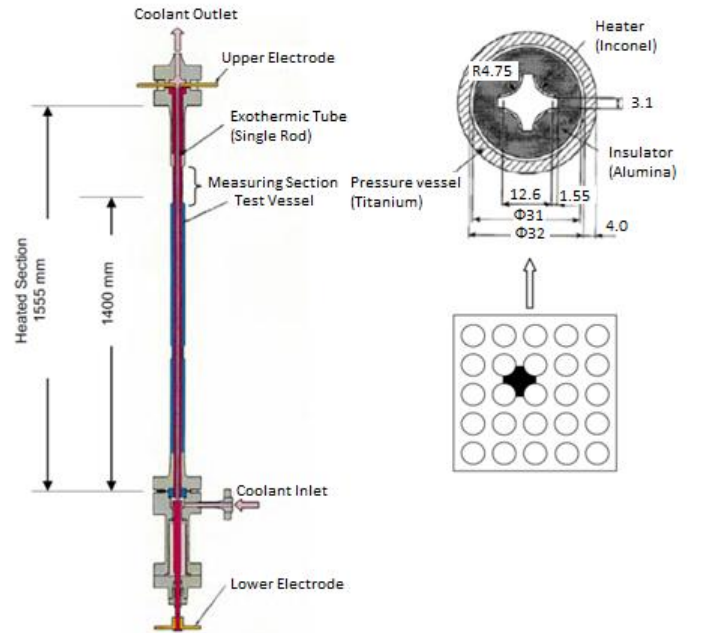


Fig. 2. Test Section for Central Sub channel Void Distribution Measurement [1].

A. Void fraction discussion

The results given by CFX and CTF were presented in Table I and it is observed that almost void fraction predicted by CFX is within error of ± 0.03 void (the value of ± 0.03 void is

also one sigma deviation of experimentally measured void fraction in single sub channel [1]). The deviation of CFX void fraction prediction is far beyond value of 0.03 with only run 1.4327 while other deviation is near 0.03.

Table I. Results of void fraction predicted by CFX and CTF

Run No	Pressure	Mass Flux	Power	Inlet Temperature	Exp.Void Fraction	CFX Results	CFX Deviation	CTF Results	CTF Deviation
	(kg/cm ²)	(10 ⁶ kg/m ² h)	(kW)	(°C)					
1.4324	100.1	5.02	60.1	238.9	0.157	0.1608 ^a	0.0038	0.197	0.040
1.1223	169.1	11	49.9	339.7	0.332	0.2836	0.0484	0.174	0.158
1.6311	50.6	1.95	20.1	204.1	0.372	0.3827 ^a	0.0107	0.308	0.064
1.2212	150.1	10.88	90	299.4	0.079	0.1208 ^a	0.0418	0.109	0.030
1.4326	100.1	5.02	60.1	268.8	0.531	0.5416	0.0106	0.555	0.024
1.6222	50	5.0	49.9	204.2	0.306	0.3432	0.0372	0.329	0.023
1.1222	169.1	10.98	50	334.7	0.142	0.1671 ^a	0.0251	0.096	0.046
1.2237	150.3	10.93	60	329.6	0.44	0.4066	0.0334	0.347	0.093
1.4311	100.4	5.01	79.9	214.2	0.215	0.2423	0.0273	0.235	0.020
1.4327	100.1	4.96	59.9	289	0.688	0.5825	0.1055	0.688	0.000
1.1221	169.1	11.0	49.9	329.7	0.087	0.1078 ^b	0.0208	0.033	0.054

(a) Kim and Park, (b) Ranz Marshall, (c) Warrier’s Nusselt correlation is applied.

For the CTF void fraction predictions, almost results are within error of ± 0.05 void. Table I shows that the CTF void fraction prediction is far beyond experiment measured data in case of runs: 1.1223, 1.2237. For these runs the CTF prediction results are nearly within error of ± 0.1 void while CFX predictions are within error of ± 0.05 .

Throughout Table I, it is observed that CFX void fraction predictions for the runs: 1.4324, 1.6311, 1.4326, 1.1222, 1.4311 and 1.1221 give error deviation smaller than ± 0.03 . These predictions are within experimentally measured one sigma deviation, so that they can

be considered to simulate experiment appropriately and can be considered as reference for comparison with CTF prediction.

Two graphs of Figure 3 shows that CTF void fraction predictions tend to under prediction with void fraction below 0.2 and, especially, the left graph of Figure 3 for all three runs with high pressure (169 kg/cm²) presents clearly the under prediction of CTF for small bubble flow.

Therefore the CTF correlations applied to small bubble regime ($\alpha_g < 0.2$) may not suitable for PWR conditions.

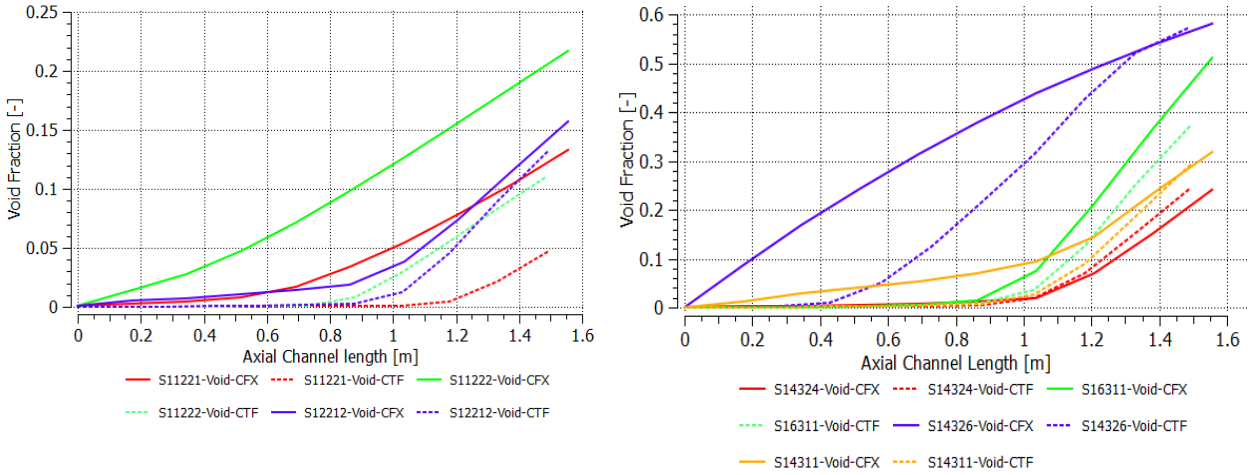


Fig. 3. Axial channel void fraction distribution predictions by CFX and CTF

The runs: 1.2237 and 1.1223 were implemented under very high pressure (169 kg/cm² for 1.1223 and 150 kg/cm² for 1.2237). So that, in such runs, the inaccuracy of CTF predictions may result from the fact that, high pressure condition similar to PWR is not appropriate to CTF heat transfer coefficient, especially in small bubble regime. The other reason may come from turbulent model. In CTF physical models, the phase change is induced from two items: (a) thermal phase change and (b) turbulent mixing and void drift. The effect of all models for phase change is still need

improved for high pressure condition similar to PWR. For the runs 1.4326, 1.2237, the experimentally measured void fraction values are above 0.4. It is observed that at the upstream, where flow in small bubble regime, CTF void fraction calculations are always under predicted, but at downstream, where flow in churn or even in annular regime, the trend of CTF void fraction calculations increases rapidly than CFX and give more accurate results in comparison with experiment. Thus, at the high void fraction, CTF may give more accurate prediction.

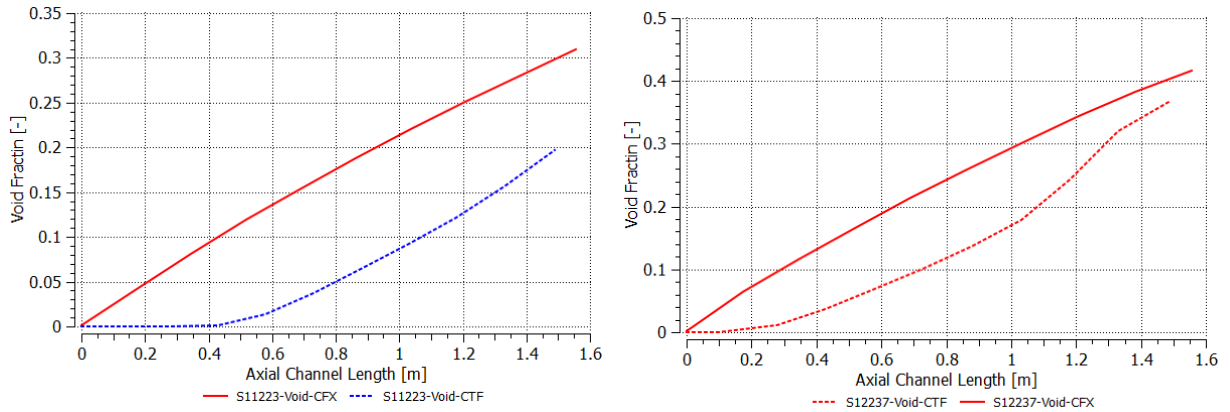


Fig.4. Axial channel void fraction distribution for runs: 1.1223 and 1.2237

B. Axial channel liquid enthalpy distribution discussion

The comparison between CFX and CTF for liquid enthalpy distribution is based on above runs that CFX give enough accurate results. These runs are: 1.4324, 1.6311, 1.4326, 1.1222, 1.4311 and 1.1221. The left graph of Figure 5 shows the axial channel liquid enthalpy distribution predicted by CTF and CFX for runs: 1.4324, 1.6311 and 1.4311. For these runs, it is obvious that the enthalpy distribution predictions are similar. However the right graph of Figure 5 shows the discrepancy between CFX and CTF for axial

channel void fraction distribution. Thus, the Chen’s correlation for these runs is acceptable but the closure models for thermal phase change need more improvement. The left graph of Figure 6 shows the axial channel enthalpy distribution calculated by CTF and CFX for the runs: 1.4326, 1.1222 and 1.1221 and it is clear that CTF gives the over prediction for liquid enthalpy distribution. The finding that CTF tend to over predict enthalpy in subcooled region is already mentioned in [4] when investigation of EPRI experiment and it is now shown the left graph of figure 6.

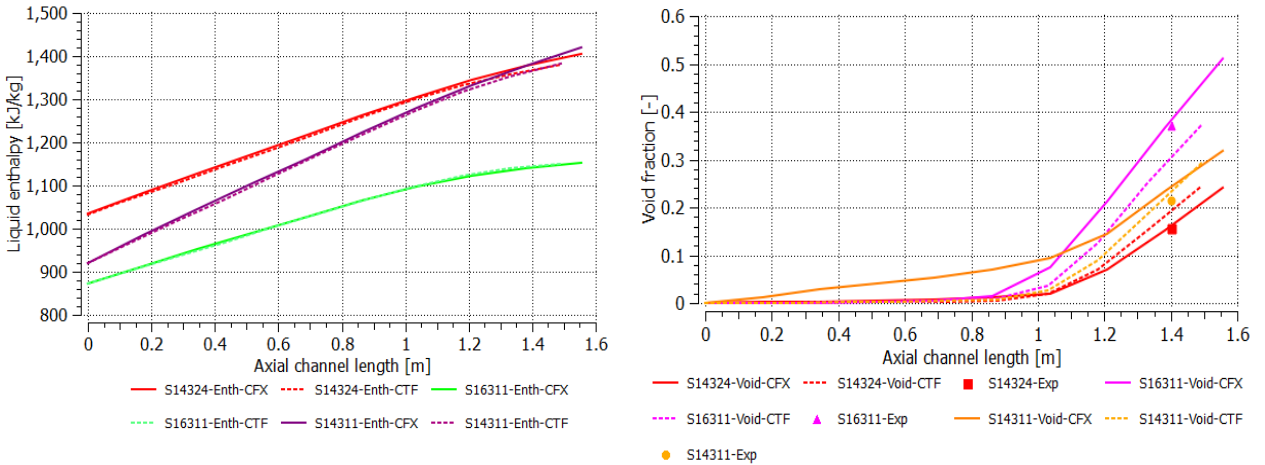


Fig.5. Axial channel enthalpy and void fraction distribution prediction by CTF and CFX for runs: 1.4324, 1.6311 and 1.4311

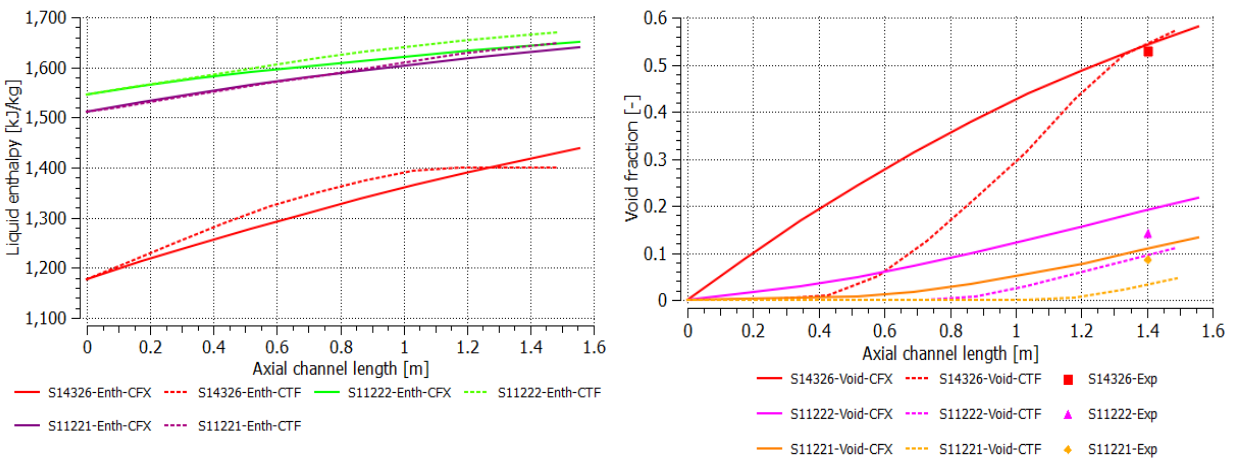


Fig. 6. Axial channel enthalpy and void fraction distribution prediction by CTF and CFX for runs: 1.4326, 1.1222 and 1.1221

When comparison of two left graphs of Figure 5 and Figure 6, the CTF over prediction for liquid enthalpy distribution occurs in the runs: 1.1222 and 1.1221 in which the pressure is very high (169 kg/cm²).

IV. CONCLUSIONS

It is summarized some findings of CTF from the study as following. CTF void fraction calculation is often under predicted where flow in small bubble regime ($\alpha_g < 0.2$). The over prediction for liquid enthalpy along axial channel occurs in case of high pressure (from 100 kg/cm² to 169 kg/cm²). CTF void fraction prediction is within error of 0.05 void when pressure not greater than 100 kg/cm². For all

investigated run in this study, the CTF void fraction prediction is within error bound of 0.1 void. CTF can give more accurate void fraction prediction in case of flow falling in churn or annular regime.

ACKNOWLEDGMENT:

The authors of this paper wish to express their appreciation for the financial support from Ministry of Science and Technology (MOST) through the National R&D Project: "Study the Nuclear Power Plant's Technology proposed for Ninhthuan 1 and Ninhthuan 2 in order to support Basic Design's Review", code KC.05.26/11-15.

Nomenclature

A	Area relevant for lateral exchange (m ²)	ρ_{ki}	Density of phase k in sub channel i (kg/m ³)
σ	Surface tension (N/m)	ρ_g	Vapor density (kg/m ³)
μ	Fluid viscosity (Pa.s)	$\bar{\rho}$	Mixing density (kg/m ³)
P	Pressure (Pa)	β_{TP}	Two phase turbulent mixing coefficient
Γ''	Evaporation rate (kg/m ² .s)	α_g, r_g	Void fraction
T _w	Wall surface temperature (K)	α_{kiEQ}	Equilibrium quality void fraction
T _{chf} , T _{crit}	Critical heat flux temperature (K)	α_{ki}	Void fraction of phase k induced by sub channel i
Re	Reynolds number	q_w'''	Volumetric heat transfer from the wall (W/m ³)
Pr	Prandtl number	q_w''	Total wall heat flux (W/m ²)
Nu	Nusselt number	q_q''	Quenching heat flux (W/m ²)
n	Wall nucleation site density (m ⁻²)	q_e''	Evaporative heat flux (W/m ²)
k _l , λ_l	Liquid thermal conductivity (W/m.K)	q_c''	Convective heat flux (W/m ²)
h _v	Vapor enthalpy (J/kg)	d_β	Local mean bubble diameter (m)
h _{nb}	Nucleate-boiling heat transfer coefficient (W/m ² .K)	T _{sat}	Saturation temperature (K)
h _l	Liquid enthalpy (J/kg)	T _l	Liquid temperature (K)
h _g	Vapor saturation enthalpy (J/kg)	S _k	Mesh-cell area of phase k (m ²)
h _{fc}	Forced-convective heat transfer coefficient (W/m ² .K)	S _{Chen}	Chen suppression factor
h _f	Liquid saturation enthalpy (J/kg)	Q _l	Heat transfer per volumetric unit (W/m ³)
h _c	Chen correlation heat transfer coefficient (W/m ² .K)	\bar{G}	Mixing mass flux (kg/m ³ .s)
g	Gravitational acceleration (m/s ²)	A _{int,shl} '''	Super-heated liquid interfacial area per unit volume (m ⁻¹)
F _{Chen}	Chen Reynolds number factor	A _{int,shv} '''	Super-heated vapor interfacial area per unit volume (m ⁻¹)
f	Bubble detachment frequency (s ⁻¹)	A _{int,scl} '''	Sub-cooled liquid interfacial area per unit volume (m ⁻¹)
D _h	Hydraulic diameter (m)	A _{int,scv} '''	Sub-cooled vapor interfacial area per unit volume (m ⁻¹)
C _p	Specific heat, constant pressure (J/kg.K)	A ₂	Area influence factors

A_x	Mesh-cell area, X normal (m ²)	$h_{int,scv}$	Sub-cooled vapor interface heat transfer coefficient (W/m ² .K)
A_s	Conductor surface area in mesh cell (m ²)	$h_{int,scl}$	Sub-cooled liquid interface heat transfer coefficient (W/m ² .K)
ΔX	Mesh-cell axial height (m)	$h_{int,shv}$	Super-heated vapor interface heat transfer coefficient (W/m ² .K)
χ_{TT}^{-1}	Inverse Martinelli factor	$h_{int,shl}$	Super-heated liquid interface heat transfer coefficient (W/m ² .K)
ρ_l	Liquid density (kg/m ³)	\dot{m}_k^{VD}	Mass exchange due to drift model (kg/s)
Fo	Fourier number	\dot{m}_k^{TM}	Mass exchange of phase k (kg/m ² .s)

REFERENCE

[1] A. Rubin et al., "OECD/NRC Benchmark Based on NUPEC PWR Sub channel and Bundle Tests (PSBT), Volume I: Experimental Database and Final Problem Specifications," US NRC / OECD Nuclear Energy Agency, pp. 12-22, November 2010.

[2] Adam Joseph Rubin., "OECD/NRC Benchmark based on NUPEC PWR Sub channel and Bundle. Tests (PSBT) - Analysis using sub channel code CTF and system code TRACE", A Thesis in Nuclear Engineering for the Degree of Master of Science, The Pennsylvania State University, May 2011.

[3] M. Avramova, A. Velazquez-Lozada, and A. Rubin., "Comparative Analysis of CTF and Trace Thermal-Hydraulic Codes Using OECD/NRC PSBT Benchmark Void Distribution Database", Hindawi Publishing Corporation, Science and Technology of Nuclear Installations, Volume 2013, Article ID 725687, pp. 2-5, Accepted 16 November 2012.

[4] Murray Cameron Thames., "Application and Assessment of a 9-equation Sub channel Methodology to Rod Bundles", A thesis in Nuclear Engineering for the Degree of Master of Science, North Carolina State University, pp. 2-6, 44-48, 2014.

[5] J. Michael Doster., "Assessment of the Performance of COBRA-TF for the Prediction of Subcooled Boiling Conditions in Rod Bundles", CASL-U-2013-0201-000, September 30, p. 24, 2013.

[6] Robert K. Salko., "Improvement of COBRA-TF for modeling of PWR cold- and hot-legs during reactor transients", A dissertation in Nuclear Engineering for the Degree of Doctor of Philosophy, The Pennsylvania State University, pp. 7-17, May 2012.

[7] Subcooled Boiling Data from Rod Bundles, EPRI, Palo Alto, CA; 2002. 1003383.

[8] S. G. Beus, "A two-phase turbulent mixing model for flow in rod bundles," Tech. Rep. WAPD-T-2438, Bettis Atomic Power Laboratory, 1970.

[9] N. Kurul and M. Z. Podowski, "On the modeling of multi dimensional effects in boiling channels", Proceedings of the 27th National heat transfer Conference, Minneapolis, July 1991.

[10] H. Anglart, O. Nylund, N. Kurul, and M. Z. Podowski, "CFD prediction of flow and phase distribution in fuel assemblies with spacers," *Proceedings of the NURETH-7*, Saratoga Springs, New York, 1995, published in: Nuclear Eng. & Design (NED), Vol. 177, pp. 215-228, 1997.

[11] G. Rabello dos Anjos, Jacopo Buongiorno., "Bubble Condensation Heat Transfer in Subcooled Flow Boiling at PWR Conditions: a Critical Evaluation of Current Correlations", Massachusetts Institute of Technology Cambridge, MA, USA, pp. 8-11, September 2013.